AFRL-AFOSR-JP-TR-2023-0037

Novel high quality GeSn alloys for mid-infrared photodetectors

Jim Williams
AUSTRALIAN NATIONAL UNIVERSITY RESEARCH OFFICE ACTON (AUSTRALIA)
10C EAST RD
ACTON, ,
AU

11/07/2022
Final Technical Report

Air Force Research Laboratory
Air Force Office of Scientific Research
Asian Office of Aerospace Research and Development
Unit 45002, APO AP 96338-5002

REPORT DOCUMENTATION PAGE

PLEASE DO NOT RETURN YOUR FORM TO THE ABOVE ORGANIZATION.

1. REPORT DATE	2. REPORT TYPE	3. DATES COVERED	
20221107	Final	START DATE 20200926	END DATE 20210925

4. TITLE AND SUBTITLE
Novel high quality GeSn alloys for mid-infrared photodetectors

5a. CONTRACT NUMBER	5b. GRANT NUMBER	5c. PROGRAM ELEMENT NUMBER
	FA2386-18-1-4078	61102F
5d. PROJECT NUMBER	**5e. TASK NUMBER**	**5f. WORK UNIT NUMBER**

6. AUTHOR(S)
Jim Williams

7. PERFORMING ORGANIZATION NAME(S) AND ADDRESS(ES)
AUSTRALIAN NATIONAL UNIVERSITY RESEARCH OFFICE ACTON (AUSTRALIA)
10C EAST RD
ACTON
AU

8. PERFORMING ORGANIZATION REPORT NUMBER

9. SPONSORING/MONITORING AGENCY NAME(S) AND ADDRESS(ES)	10. SPONSOR/MONITOR'S ACRONYM(S)	11. SPONSOR/MONITOR'S REPORT NUMBER(S)
AOARD UNIT 45002 APO AP 96338-5002	AFRL/AFOSR IOA	AFRL-AFOSR-JP-TR-2023-0037

12. DISTRIBUTION/AVAILABILITY STATEMENT
A Distribution Unlimited: PB Public Release

13. SUPPLEMENTARY NOTES

14. ABSTRACT
Intense research interest in GeSn alloys in recent years has been fuelled by their potential for efficient light absorption in the near-to-mid infrared (IR), the possibility of mid-IR lasers, and their ready compatibility, including integration with Si fabrication. This project, which has been a 3 way collaboration between ANU, AFRL at Wright Patterson Labs, and ARDEC Benet Labs, has focussed on three areas: i) full characterisation at ANU of a range of CVDgrown structures from AFRL on both Ge and Si substrates; ii) production of GeSn and GePb alloys on Ge substrates by a combination of ion implantationat ANU and pulsed laser melting (PLM) at ARDEC; iii) use of implantation/PLM to dope CVD-grown GeSn films, and to try to reduce the defect density in relaxed CVD-grown GeSn films grown on Si. Despite the impact of COVID, and COVID-induced lockdown of laboratories, considerable significant achievements have been achieved in all 3 projects areas. In area i) CVD-grown GeSn layers on Si of various Sn content have been fully assessed, and a publication is in the final stages of preparation. A range of superlattice structures have been successfully characterised by ion channelling (RBS-C) and electron microscopy (TEM): with some further TEM, a publication will be possible. In area ii), a publication on relaxed GeSn layers produced by ion implantation/PLM has been published, and the first dilute GePb films have produced. The latter results can be published with a little further TEM analysis. In the third area, both the Intense research interest in GeSn alloys in recent years has been fuelled by their potential for efficient light absorption in the near-to-mid infrared (IR), the possibility of mid-IR lasers, and their ready compatibility, including integration with Si fabrication. This project, which has been a 3 way collaboration between ANU, AFRL at Wright Patterson Labs, and ARDEC Benet Labs, has focussed on three areas: i) full characterisation at ANU of a range of CVDgrown
structures from AFRL on both Ge and Si substrates; ii) production of GeSn and GePb alloys on Ge substrates by a combination of ion implantationat ANU and pulsed laser melting (PLM) at ARDEC; iii) use of implantation/PLM to dope CVD-grown GeSn films, and to try to
reduce the defect density in relaxed CVD-grown GeSn films grown on Si. Despite the impact of COVID, and COVID-induced lockdown of laboratories, considerable significant achievements have been achieved in all 3 projects areas. In area i) CVD-grown GeSn layers on
Si of various Sn content have been fully assessed, and a publication is in the final stages of preparation. A range of superlattice structures have been successfully characterised by ion channelling (RBS-C) and electron microscopy (TEM): with some further TEM, a publication will be possible. In area ii), a publication on relaxed GeSn layers produced by ion implantation/PLM has been published, and the first dilute GePb films have produced. The latter results can be published with a little further TEM analysis. In the third area, both the implant/PLM doping and attempts to reduce GeSn layer defect levels have proven problematic. However, the impediments to successful implementation of this approach have been identified and an improved design of these experiments should be successful in the future. Finally, further work is planned to progress, extend and complete this project, with a new AOARD project recently applied for, that, if successful, will begin in 2022.

15. SUBJECT TERMS

16. SECURITY CLASSIFICATION OF:			17. LIMITATION OF ABSTRACT	18. NUMBER OF PAGES
a. REPORT U	b. ABSTRACT U	c. THIS PAGE U	SAR	17
19a. NAME OF RESPONSIBLE PERSON TONY KIM			19b. PHONE NUMBER *(Include area code)* 315-227-7008	

Standard Form 298 (Rev.5/2020)
Prescribed by ANSI Std. Z39.18

AOARD Proposal 18IOA078

Final project report 17 December 2021

Project Title: Novel high quality GeSn alloys for mid-infrared photodetectors

Principal Investigator: Professor Jim Williams, Emeritus Professor
Department of Electronic Materials Engineering
Research School of Physics and Engineering
Australian National University (ANU)
Mills Rd., Canberra 2601 Australia
Ph: +61261250373
Fax: +61261250511
Email: Jim.Williams@anu.edu.au

Co-Principal Investigator: Dr. Bruce "Chip" Claflin
Senior Research Physicist
Electro-Optics/Infrared Components Branch Air Force Research Laboratory
2241 Avionics Circle
Wright-Patterson, AFB OH 45433
ph: (937) 713-8740
fax: (937) 255-6942
Email: bruce.claflin.1@us.af.mil

Project Summary:

Intense research interest in GeSn alloys in recent years has been fuelled by their potential for efficient light absorption in the near-to-mid infrared (IR), the possibility of mid-IR lasers, and their ready compatibility, including integration with Si fabrication. This project, which has been a 3 way collaboration between ANU, AFRL at Wright Patterson Labs, and ARDEC Benet Labs, has focussed on three areas: i) full characterisation at ANU of a range of CVD-grown structures from AFRL on both Ge and Si substrates; ii) production of GeSn and GePb alloys on Ge substrates by a combination of ion implantationat ANU and pulsed laser melting (PLM) at ARDEC; iii) use of implantation/PLM to dope CVD-grown GeSn films, and to try to reduce the defect density in relaxed CVD-grown GeSn films grown on Si. Despite the impact of COVID, and COVID-induced lockdown of laboratories, considerable significant achievements have been achieved in all 3 projects areas. In area i) CVD-grown GeSn layers on Si of various Sn content have been fully assessed, and a publication is in the final stages of preparation. A range of superlattice structures have been successfully characterised by ion channelling (RBS-C) and electron microscopy (TEM): with some further TEM, a publication will be possible. In area ii), a publication on relaxed GeSn layers produced by ion implantation/PLM has been published, and the first dilute GePb films have produced. The latter results can be published with a little further TEM analysis. In the third area, both the implant/PLM doping and attempts to reduce GeSn layer defect levels have proven problematic. However, the impediments to successful implementation of this approach have been identified and an improved design of these experiments should be successful in the future. Finally, further work is planned to progress, extend and complete this project, with a new AOARD project recently applied for, that, if successful, will begin in 2022.

1. Revised Project Objectives:

The overall objective of this proposal was to develop high quality GeSn alloy materials that are suitable for fabricating efficient near-to-mid infrared photodetectors (at wavelengths beyond 4 μm) at room temperature. Two non-equilibrium approaches were used to produce such materials at Sn concentrations that substantially exceed the solid solubility limit of Sn in Ge. First, alloys of varying thickness and composition grown by CVD on both Ge and Si substrates have been fully assessed by a number of advanced techniques both at ANU and AFRL. Investigations were carried out on these CVD-grown films to determine if a combination of ion implantation/pulsed laser melting (PLM) could be employed in an attempt to both selectively remove grown-in defects and to introduce dopants into the materials. Second, GeSn films were fabricated by a combination of ion implantation (at ANU) and PLM (at the ARDEC Benet Labs), to produce thin films of GeSn of varying compositions on both Ge and Ge on Si substrate structures. An array of advanced characterisation techniques was used to analyse and compare the various alloy films. In addition, a preliminary investigation was carried out to assess if GePb alloys of compositions up to around 1 atomic % could be achieved by a combination of ion implantation/PLM.

Specific objectives for year 3

- Complete physical characterisation of CVD grown GeSn layers on Si. If possible, complete and submit a manuscript for publication on characterisation of various compositions of GeSn grown on Si.
- Further attempts to be made to successfully implement the PLM re-melting strategy on CVD GeSn grown on Si in an attempt to reduce defect density. However, this will rely on the availability of thicker GeSn films, greater than about 800 nm.
- Assess the data to date on CVD-grown superlattices on both Ge and Si and undertake any further work that is required to publish it (including annealing to fully relax the films). Certainly, further TEM will be required to eliminate the FIB damage in existing TEM samples.
- Undertake preliminary electrical measurements on existing Sb implanted (and PLMed) structures to determine, if possible, whether a p-n junction has formed. Use this data to design further doping schemes for photodetector device structures.
- Examine if Raman mapping can be used to obtain a measure of the defect density from peak shifts and undertake etching studies to correlate defect density with depth.
- Implant Pb into Ge at a range of doses (Pb concentrations) and carry out PLM to assess whether it is possible to trap Pb into substitutional locations during rapid solidification. If successful, use this method to plan future research to produce GePb layers on both Ge and Si substrates.

2. Project achievements with a focus on year 3:

In this final report, the results for years 1 and 2 are summarised, and the results during year 3 are given in more detail. It must be stressed that a number of COVID lockdowns over the course of this project significantly impacted on the overall research progress. Nevertheless, significant results and achievements have resulted that can be the

basis for further work if a new project grant is approved. A new grant would allow for a substantially expanded program with more ambitious project goals.

The following section summarises the results in years 1 and 2.

2.1. Highlights of results during years 1 and 2

2.1.1 Characterisation of CVD-GeSn films grown on Si.

Four different compositions were examined, covering the range nominally from 2-10 at% Sn. Rutherford backscattering and channelling and TEM were the main characterisation tools undertaken during years 1 and 2. A comparison of the data from these methods with XRD data taken at AFRL was carried out.

A summary of the RBS and channeling data is given in Fig. 1. In each panel the partial RBS (and channeling) spectra for each nominal composition is shown, with the best fit simulations shown in orange. Note that, for 3 MeV He ion beam analysis, the Ge and Sn signals are well separated for the two highest Sn composition films but not for the other two cases. The Sn composition of the films was found to be 3.5%, 5%, 7% and 11%, compared with the nominal film thicknesses from XRD of 4%, 4.7%, 7%, and 10.6%. Hence, the RBS and XRD results are in good agreement, as were the measured film thicknesses. Indeed, for all cases, the RBS simulation data was within 10% of the nominal composition and thickness values. Furthermore, the channeling results (channeling minimum yields) indicate defective single crystalline GeSn films, with the defect density increasing with Sn composition as expected. The disorder is maximum near the Ge-GeSn interface and reduces towards the surface.

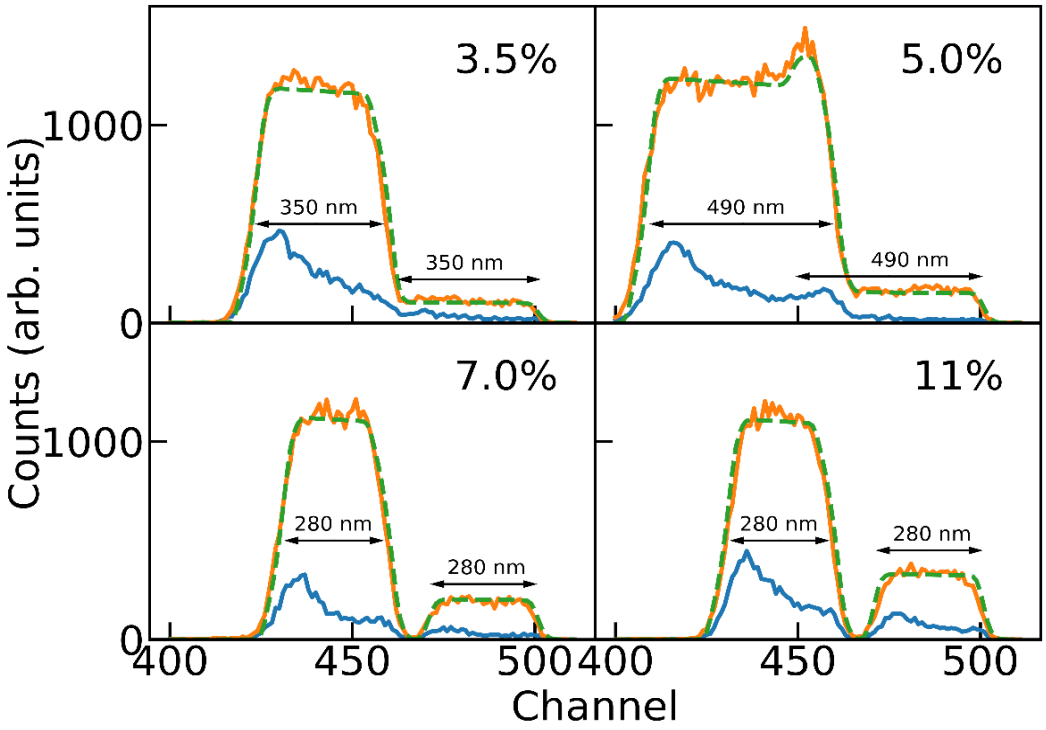

Fig. 1*. Collage of different Sn content GeSn films showing partial RBS and channeling spectra of the Sn and Ge parts of each spectrum. The best fit simulations are also shown by the dashed green curves, and the compositions and film thicknesses found from the simulations are indicated in each case.*

Cross-sectional TEM of all samples showed a high density of threading defects emanating from the GeSn-Si interface, as illustrated in Fig. 2. These defects are associated with lattice mismatch between the Si substrate and the GeSn films, and increase in density with Sn composition, consistent with the channeling data. Furthermore, it was found that the defect density was greatest close to the film-Si interface and decreased closer to the surface, again in agreement with the channeling data. In short, these data indicate that the films are either fully or partially relaxed. High resolution TEM was also undertaken on these samples, including convergent beam characterization, as well as measurements of the lattice parameter of the films, to determine possible residual strain in each GeSn film.

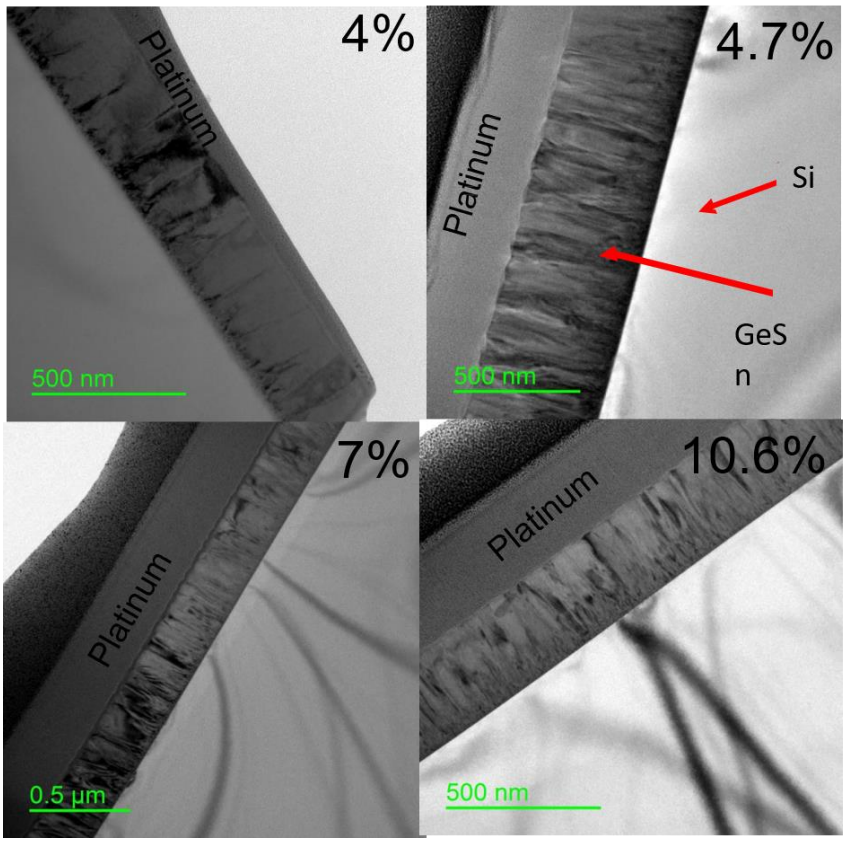

Fig. 2. *A collage of cross-sectional TEM micrographs of the various compositions.*

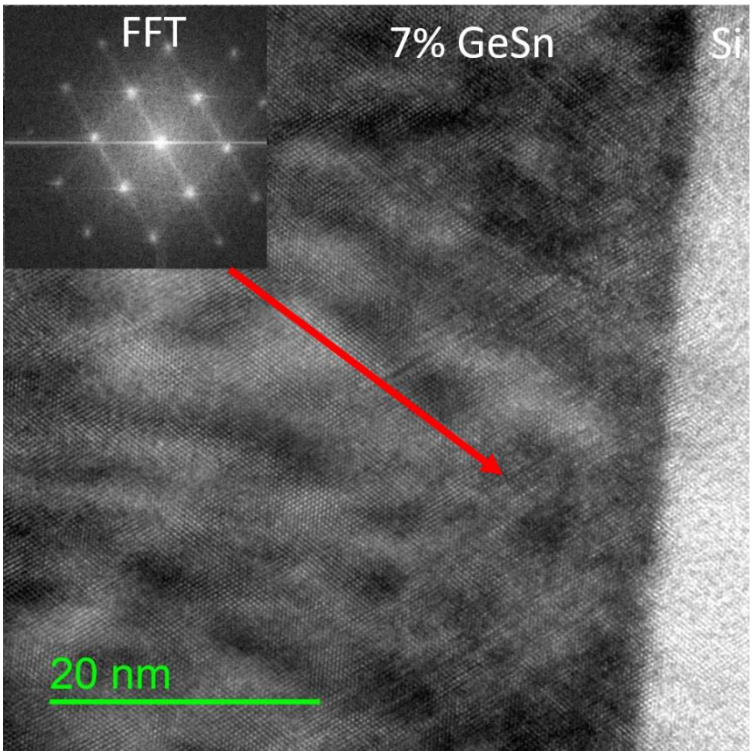

Fig. 3. *High resolution TEM micrograph close to the interface of the 7% Ge Sn film with a selected area fast Fourier transform diffraction pattern.*

The lattice parameter for each composition, taken from high resolution diffraction data such as that in Fig. 3, was found to fit on the line of full relaxation for the 3.5%, 5% and 11% films compositions. This suggests that these compositions were fully relaxed, as expected. However, the 7% film was not fully relaxed, and contained a small amount of compressive strain, probably since this was the thinnest layer. Note also the line defects along <111> directions in Fig 3, that emanate from the interface and result from film relaxation.

The Raman data (peak shifts) for these film compositions was also consistent with the lattice parameter data from RBS/channelling, TEM and XRD. Indeed, the level of agreement in terms of film thickness, film composition and lattice parameter (strain) between the measurements at AFRL (from XRD and in-situ data) and measurements at ANU (from RBS, TEM and Raman) are in excellent agreement. Furthermore, the ANU measurements were able to provide the level of defects, as well as the defect distribution that were not available from AFRL data.

2.1.2. GeSn layers produced by ion implantation and PLM

A parallel series of studies were undertaken on Sn implanted Ge samples subsequently treated with pulsed laser melting (PLM) for both thin samples (less than about 120 nm), which appeared to exhibit residual compressive strain, and thicker layers which initially appeared to be strain-free. As an example, Fig. 4 shows the XRD data from a GeSn film prepared with an implant dose of 6×10^{16} cm^{-2} at a Sn energy of 350 keV and then subjected to PLM using a 6 ns frequency-tripled Nd:YAG laser at a fluence of 0.55 Jcm^{-2}. This sample had a nominal Sn concentration of around 6% as measured by RBS and channelling, and a Sn substitutionality of around 75%.

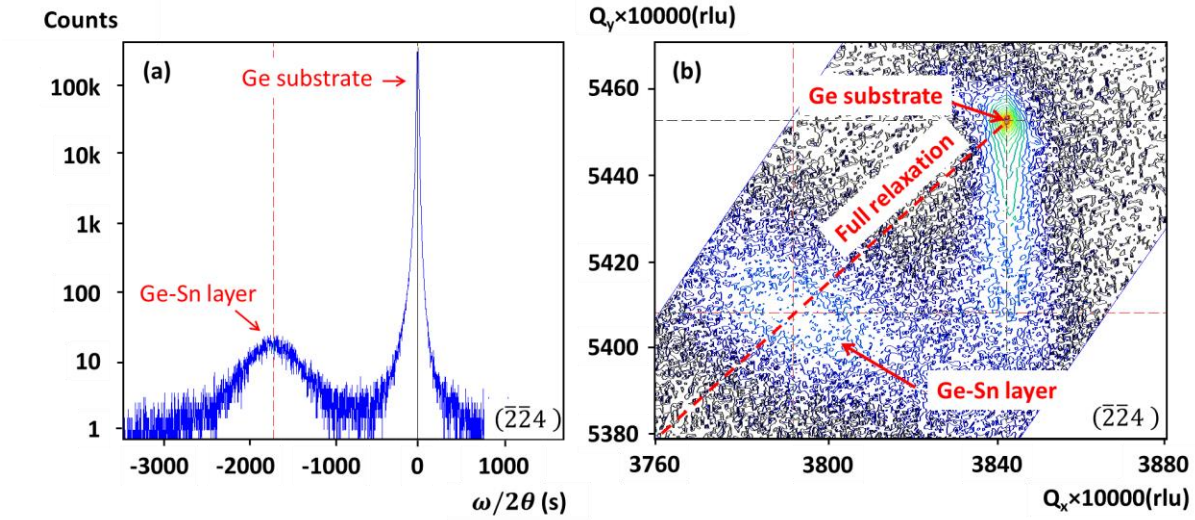

Fig. 4. *XRD-$\omega/2\theta$ scan (a) and reciprocal space mapping (b) on the $(\bar{2}\bar{2}4)$ planes of the nominally 6% Sn sample.*

In the left panel of Fig. 4, an XRD-$\omega/2\theta$ scan on the asymmetric $(\bar{2}\bar{2}4)$ planes of the nominally 6% Sn sample is shown. Due to the lattice expansion, a single XRD peak from the GeSn layer is at a lower Bragg angle than for Ge. In Fig. 4(b), reciprocal space mapping was employed to fully characterize the lattice parameters of the alloy. The most noteworthy feature in this figure is

that the GeSn peak is located along a diagonal line which indicates a near-fully-relaxed alloy. From the reciprocal space map, the lattice parameter of the GeSn layer was found to be 5.69 Å, which corresponds to a Sn composition of around 5% and close to the substitutional composition measured by RBS.

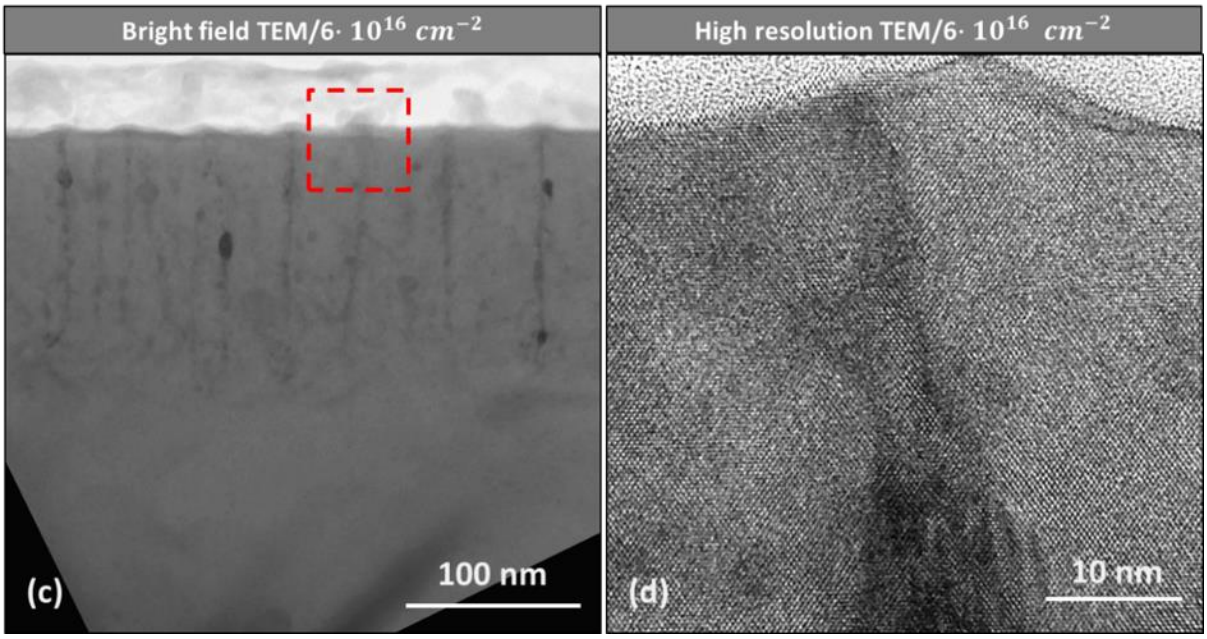

Fig. 5. *TEM cross-sectional micrographs of the nominally 6% Sn content alloy prepared by implantation and PLM. The micrograph in (a) shows 'threading-like' defects from 110 nm out to the surface, and the high-resolution image in (b) shows a well-ordered crystal and surface humps around the defects at the surface.*

Cross-sectional TEM micrographs, taken of the nominal 6% Sn sample to examine defects associated with structural relaxation, are shown in Fig. 5. In Fig. 5(a), the crystal is shown to be of high quality with vertical defects propagating out to the surface. The high-resolution cross-section of this sample (Fig. 5(b)) confirms the highly ordered arrangement of the crystal columns. The defects are in the form of thin vertical threads extending from a depth of around 110 nm to the sample surface. At the end of the threads on the surface are small bumps that appear to be an extrusion of the alloy out from the surface. The origin of these extruding defect threads is unclear. They are not conventional misfit dislocations that are associated with strain relaxation under thermal equilibrium conditions at elevated temperatures because the non-equilibrium PLM process does not give enough time for them to develop at elevated temperature. Such non-equilibrium relaxation and associated defect generation occurs to accommodate the larger GeSn lattice parameters for growth on a Ge substrate. During year 2, this implant/PLM data for production of relaxed GeSn layers was published [1].

2.1.3 Attempts to remelt defective layers to reduce the defect density

There were several attempts to use implantation into relaxed GeSn alloys and subsequent PLM to try to reduce the defect density. The experiment involved amorphising the top half of the GeSn film with Ge ions, followed by PLM that just melted beyond the amorphous layer but not up to the GeSn-substrate interface. Unfortunately, all of these attempts failed for various reasons: such as the amorphous layer was too shallow or too deep, or the PLM appeared to melt beyond the GeSn-Si interface. This experiment has also

been frustrated by a few issues: the downtime of the PLM system for an extended period of time, the effect that COVID has had on limited access to laboratories during 2020 and 2021. However, the main problem was that the thickness of the GeSn films (whether produced by CVD or by implant/PLM), was too thin to easily facilitate this experiment. It was decided in mid-2021 that substantially thicker GeSn films were needed to facilitate this experiment but it was not possible to complete this work before the end of the current project, as a result of an extended COVID lockdown at ANU.

2.1.4. Initial progress on doping layers with implantation and PLM

The purpose of this study was to fabricate an n+ top layer on a GeSn film using a shallow Sb implant and subsequent PLM. This was initially carried out on an 800 nm 4.6% GeSn layer grown on Ge. It was expected that the Sb layer would be in the top 1/3rd of the film but the amorphous implant layer actually extended more than half way across the film thickness. PLM was then undertaken at a range of fluences that should have covered the optimum fluence for just melting beyond the amorphous layer. However, although subsequent RBS/channeling measurements showed that two PLM fluences (0.5 and 0.6 J/cm^2) caused melting beyond the amorphous layer thickness, there was considerable disorder in the recrystallized GeSn film. From RBS alone, it was not possible to say how these defects arose, or even whether the melt had penetrated to the underlying substrate. TEM data, subsequently obtained just beyond the end of year 2, was inconclusive: it was not clear whether part of the laser had melted through to the underlying substrate or not. As a result, there was a considerable defect level in the film, indicating that this sample was not ideal for electrical measurements. Despite this, electrical measurements were planned for year 3 but could not be completed due to COVID lockdowns. It was decided recently to repeat this experiment with appropriate control samples beyond the project end.

2.1.5. CVD-grown superlattice characterisation

Two superlattices were examined by RBS and TEM, one being 6 GeSn-Ge layers grown on Ge, and the other being 20 GeSn-Ge layers grown on Si. Fig. 6 is a cross-sectional TEM micrograph of the 6-layer superlattice grown on Ge. Note that, unfortunately, the top two layers were amorphized during FIB sample preparation. However, the individual layers are clearly apparent and contain little damage. Hence, the individual superlattice layers are almost certainly strained layers on the underlying Ge substrate.

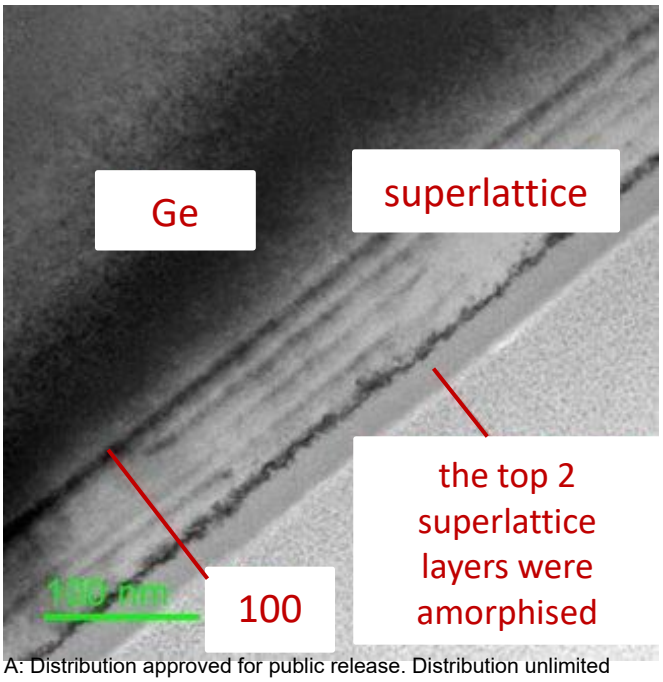

Fig. 6. *TEM cross-section of the x6 GeSn-Ge superlattice grown on Ge.*

The TEM analysis indicates that the individual layers are around 18 nm thick, which is in good agreement with the RBS data.

The RBS/channelling and TEM on the second superlattice gave similarly informative data on the thickness and quality of the individual layers, although again the TEM cross-sections contained a near-surface amorphous layer as a result of the sample preparation for TEM. It was decided that this experiment would be repeated beyond the project end, where it was expected that a paper could be written up for publication.

2.2 Details of results during year 3.

2.2.1. Recap of re-melt experiment and n-type doping with Sb

As indicated in the previous section, both the experiment to try to reduce defect density by PLM melting and the Sb doping experiment relied on melting part of an existing GeSn film on either a Si or Ge substrate. These experiments are problematical and require considerably thicker GeSn layers than those used to date. During year 3, there were further PLM attempts to partly melt GeSn layers and analyse the resulting defect structure following PLM. None of these studies have been successful. It has been decided to completely redesign these experiments in studies beyond this current project using a number of control samples to determine the differences in melt depth in GeSn layers of different composition compared with Ge substrates. For the Sb implant and PLM doping study, again implanting Sb into Ge and also GeSn layers of different composition will be examined. Finally, using CVD-grown GeSn layers considerably thicker (around 1µm) than those used to date will be needed. For the implanted Sn in Ge study, during year 3, higher Sn energies to provide thicker GeSn layer was attempted, and results will be reported below in Section 2.2.3.

2.2.2 Raman studies and mapping.

Raman analysis and mapping were carried out on several CVD-grown compositions to ascertain whether Raman could be a suitable rapid characterization method to detect defects and uniformity of GeSn layers on Si and Ge substrates. Fig. 7 shows Raman spectra for a 11% Sn content GeSn layer grown on Si. The right panel shows the dominant Ge-Ge bonding peak and indicates slight broadening which can be correlated with defects observable in TEM (see Fig. 2).

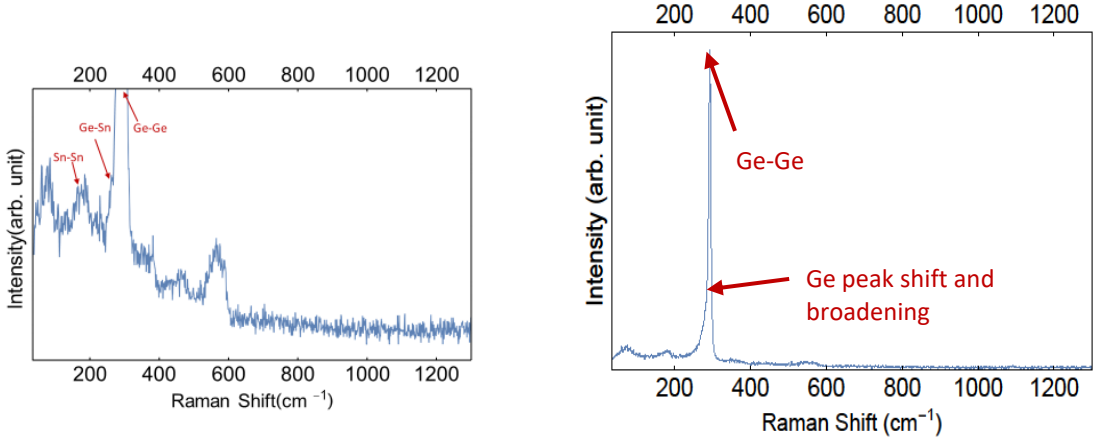

Fig. 7. *Raman spectrum from a 11% Sn content GeSn film grown by CVD on Si, showing the dominant peak and broadening (right panel) and an expanded region showing Ge-Sn and Sn-Sn bonding peaks.*

The left panel shows an expanded region of the spectrum and shows the dominant Ge-Ge peak as well as a Ge-Sn peak (shoulder) from the GeSn film, and a Sn-Sn bonding peak from Sn precipitates observed on the sample surface. The intensity of all of these features can be mapped successfully, however, the uniformity of the sample was sufficiently good that only small variations in these peaks was observed in the map (not shown).

2.2.3. Defects in implanted/PLM GeSn layers and comparison with CVD GeSn

With GeSn layers produced by ion implantation and PLM, the defects that resulted from relaxation of films thicker than about 120 nm appeared significantly different to the near-equilibrium misfit dislocations that accompany relaxation of CVD-grown alloys. Thus, a series of thicker ion implanted/PLM films were produced at a range of compositions up to around 10% Sn for better comparison defects in CVD-grown layers. Such films were also significantly thicker than those previously produced and at a higher Sn content. Hence, it was essential that the Ge substrate was capped with a sufficient thickness of SiO_2 prior to implantation, and that the cap could be completely removed prior to PLM. Fig. 8 shows RBS and channelling spectra that illustrate successful capping and removal of the cap. It turns out that, for 400 keV Sn implantation to doses in excess of $5x10^{16}$ cm^{-2}, a cap of between 50 and 60 nm is needed. The black channelled spectrum in Fig. 8 is after cap deposition onto Ge and shows the prominent Si and O peaks and the underlying Ge surface. RBS similation gives a cap thickness of 52 nm. The red spectrum shows the successful removal of the cap with HF etching, leaving no traces of SiO_2, an ideal situation for PLM.

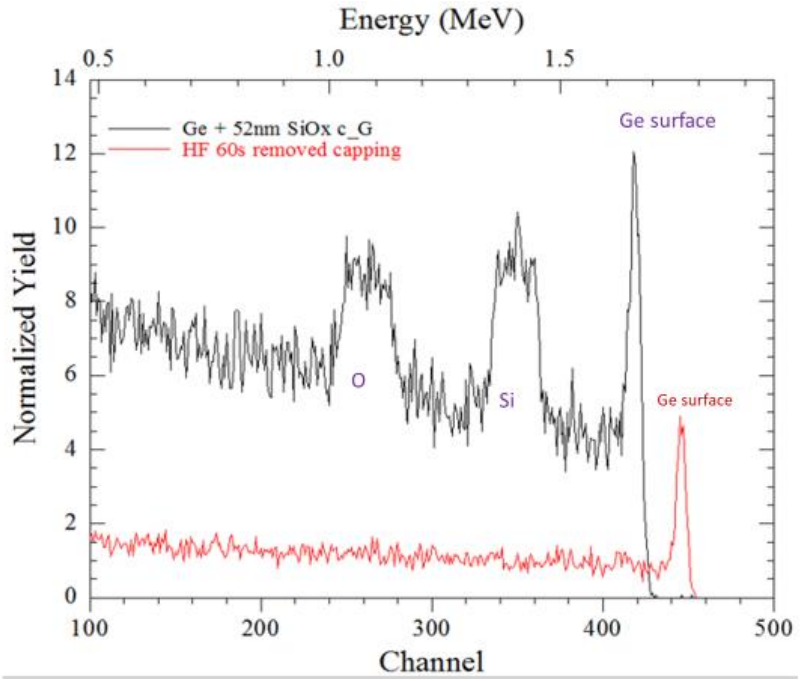

Fig. 8. *RBS channeling spectra showing a Ge sample with 52 nm of deposited SiO_2 for implantation processing (black spectrum), and with the SiO_2 layer removed by HF etching (red spectrum).*

Following cap deposition, various doses of Sn up to $6x10^{16}$ cm^{-2} were implanted into the Ge at an energy of 400 keV, to give subsequent GeSn layer thicknesses of around 400 nm. After cap removal, all samples were then subjected to PLM at various fluences to melt and crystallise the GeSn layer epitaxially on the underlying substrate. All samples were then analysed by RBS and channelling to determine the quality of the crystalline GeSn alloy and to measure the substitutional Sn content. In Fig. 9, a typical set of RBS/channeling spectra is shown for a Sn dose of $6x10^{16}$ cm^{-2}. The blue channeled spectrum is for an as-implanted sample following cap removal and shows an amorphous layer of around 390 nm resulting from the implantation. Also shown, is the as-implanted Sn profile where the peak Sn concentration is just above 10 atomic %. The red and black curves are the channeled and random spectra, respectively, after PLM, and show that a GeSn alloy has crystallised epitaxially on Ge. The Sn substitutionality is above 90%, and there is clearly some residual disorder in the alloy layer, as determined by comparison with the Ge reference (channeled) spectrum (pink curve). However, TEM is needed to determine the precise nature of this residual disorder.

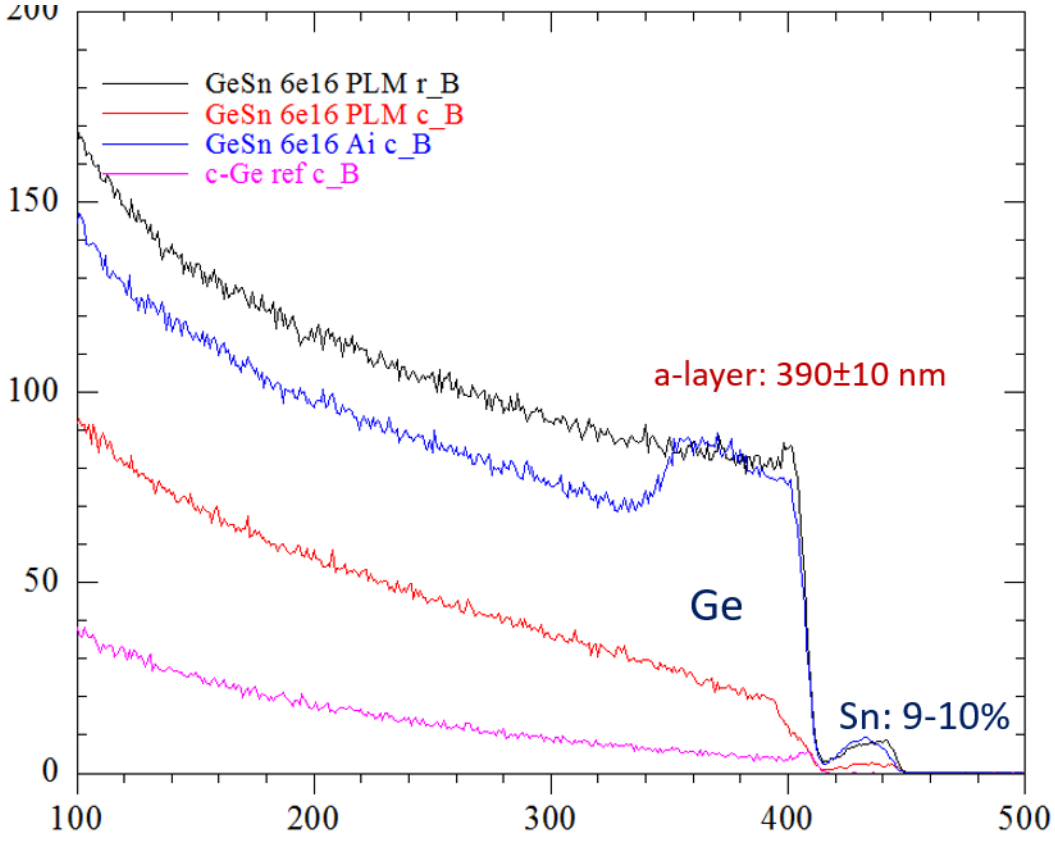

Fig. 9. *RBS random and channelled spectra for a $6x10^{16}$ cm^{-2} implant into Ge before and after PLM, showing: a channelled spectrum for a Ge reference sample (pink); a channelled spectrum after implantation (blue); a random spectrum after PLM (black); and a channelled spectrum after PLM (red).*

Fig. 10 shows a bright field cross-sectional TEM micrograph of a $6x10^{16}$ cm^{-2} Sn implant dose into Ge after PLM. Several interesting features are observed. First, at a depth of around 400 nm there is a row of defect clusters. These are close to the expected melt depth and may indicate some residual implantation damage in the Ge just below the maximum melt depth. Indeed, the laser fluence used was sufficient to melt through amorphous Ge but may have been insufficient to melt the underlying Ge crystal, which requires a slightly higher fluence threshold. The second feature of note are the line defects in the alloy that emanate from the maximum melt depth, which also signifies the GeSn-Ge interface. These defects, some of which propagate to the surface, have been previously observed in implant/PLM-produced GeSn layers (see Fig. 5) but never in such thick GeSn layers. These defects are not conventional misfit dislocations as we indicated in a previous section. Note that the GeSn composition in Fig. 10 is very close to that of the 10.6% CVD-grown film in Fig. 2, which shows typical misfit dislocations. It is clear that the implant/PLM defects that result from relaxation of GeSn are not only different to misfit defects, but the defect density is much lower, albeit that the CVD-GeSn alloy was grown on Si. A third feature of interest is the increased disorder in the near-surface 100 nm. Here, there are a number of defect clusters or second phase precipitates (white blobs). These regions are not precipitated Sn (which would appear darker than the alloy under the imaging conditions used). They are most probably a result of recoiled Si and O that occurred during implantation through the SiO_2 cap, as has been observed previously [1]. These features can be eliminated by reactive ion etching of the surface 10-15 nm of the implanted sample prior to PLM. This extra step was not carried out in the case of the sample in Fig. 10. Despite these near-surface defects, the degree of crystallinity and low defect density is very encouraging. Samples such as that illustrated in Fig. 10 would appear to be ideal for re-melting of the top ½ of the film to see if the defect density can be further reduced.

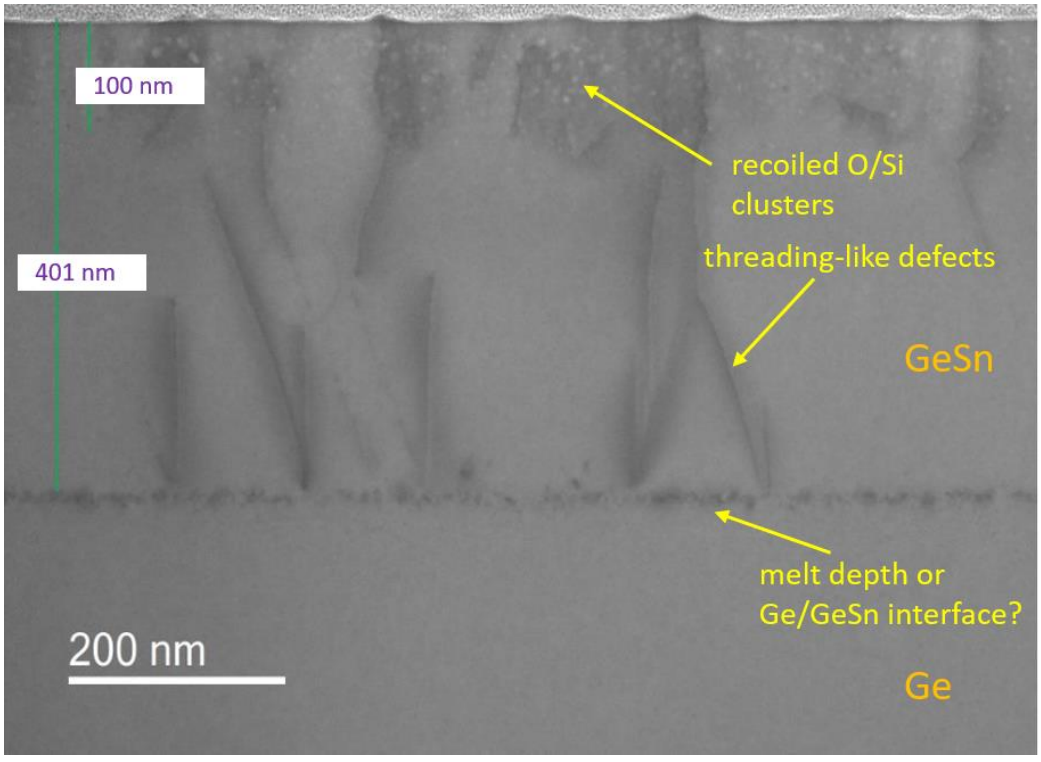

Fig. 10. *Cross-sectional TEM micrograph of a 6x10^{16} cm^{-2} implant into Ge at 400 keV after PLM.*

2.2.4 Attempts to fabricate GePb alloys by implantation/PLM

A series of experiments was carried out to assess the feasibility of producing GePb alloys by implanting Pb into Ge and then carrying out PLM, as for the GeSn case. The first challenge was to establish whether a Pb ion beam of sufficient current could be obtained at around 800 keV from the ANU ion implanter. It turned out that a method was developed to achieve a sufficient beam current for Pb concentrations up to a few atomic %. A series of Pb doses was then implanted into capped Ge at 800 keV. The next challenge was to establish if Pb could be trapped in solid Ge during solidification of the melt during PLM. Since there were no measurements in the literature for the equilibrium solid solubility of Pb in Ge, it was possible that, if the Pb solubility was extremely low, essentially all of the Pb would be 'zone refined' to the surface during melt solidification. Thus, a series of different implant-concentration samples were subjected to PLM. Fig. 11 shows RBS/channelling spectra for a case of a Pb dose of 1x10^{15} cm^{-2} at 800 kV before and after PLM (after SiO_2 cap removal). The blue curve is a channelled spectrum after implantation showing an amorphous layer of around 410-420 nm, and the as-implanted Pb profile in the magnified insert. After PLM, the channelled curve (red) is almost identical to the Ge reference (pink curve) and this indicates that there are likely to be few residual defects in an excellently crystallised implanted layer. From the insert, comparing the Pb profiles in the channelled (red) spectrum and the random (black) spectrum, indicates that about half of the Pb is segregated to the surface during PLM, but the Pb trapped in the solid is substantial and almost 100% substitutional. This is an encouraging result since, in this case, a GePb alloy of around 0.5% Pb content has been produced.

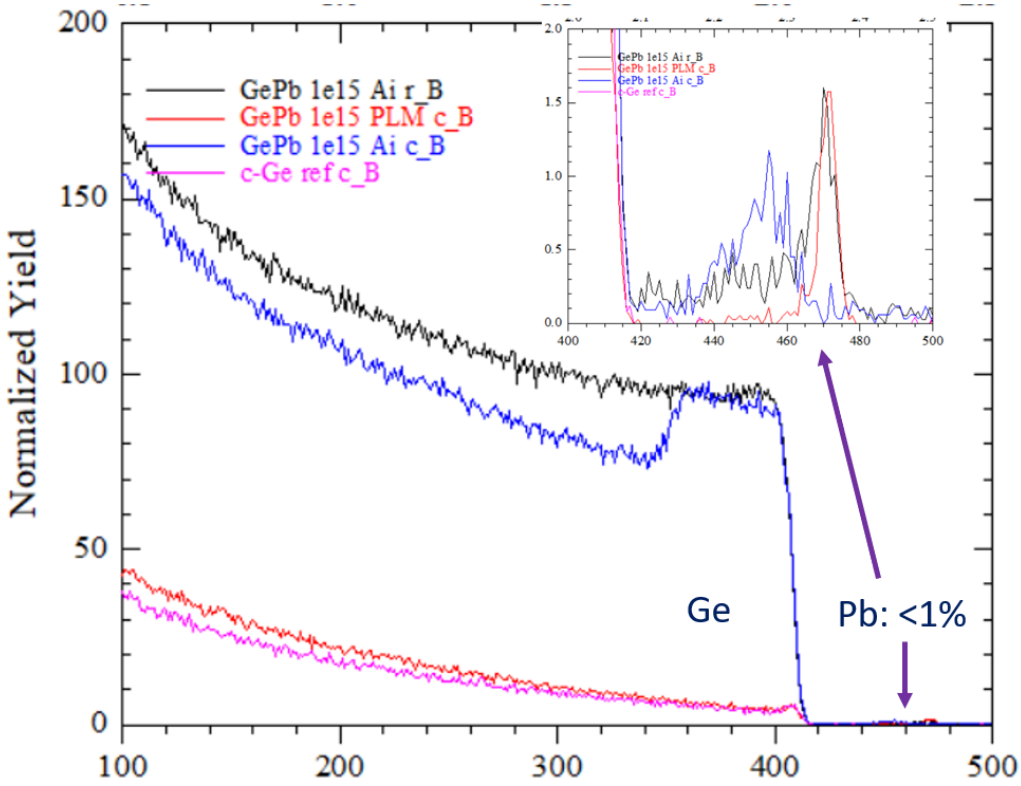

Fig. 11. *RBS random and channelled spectra for a 1x10^{15} cm^{-2} Pb implant into Ge at 800 keV before and after PLM, showing: a channelled spectrum for a Ge reference sample (pink); a channelled spectrum after implantation (blue); a random spectrum after PLM (black); and a channelled spectrum after PLM (red). The insert shows a magnified region of the Pb profiles for each spectrum.*

To establish if the GePb alloy illustrated in Fig. 11 is indeed defect-free, TEM is needed. In Fig. 12, a cross-sectional bright field TEM micrograph is shown that is essentially featureless. However, it is possible to observe a faint line at the expected maximum depth of the melt front (just beyond the amorphous layer depth). Thus, the TEM confirms the near-perfect quality of the dilute (0.5%) GePb alloy produced. To our knowledge, this is the first time that such an alloy has been produced.

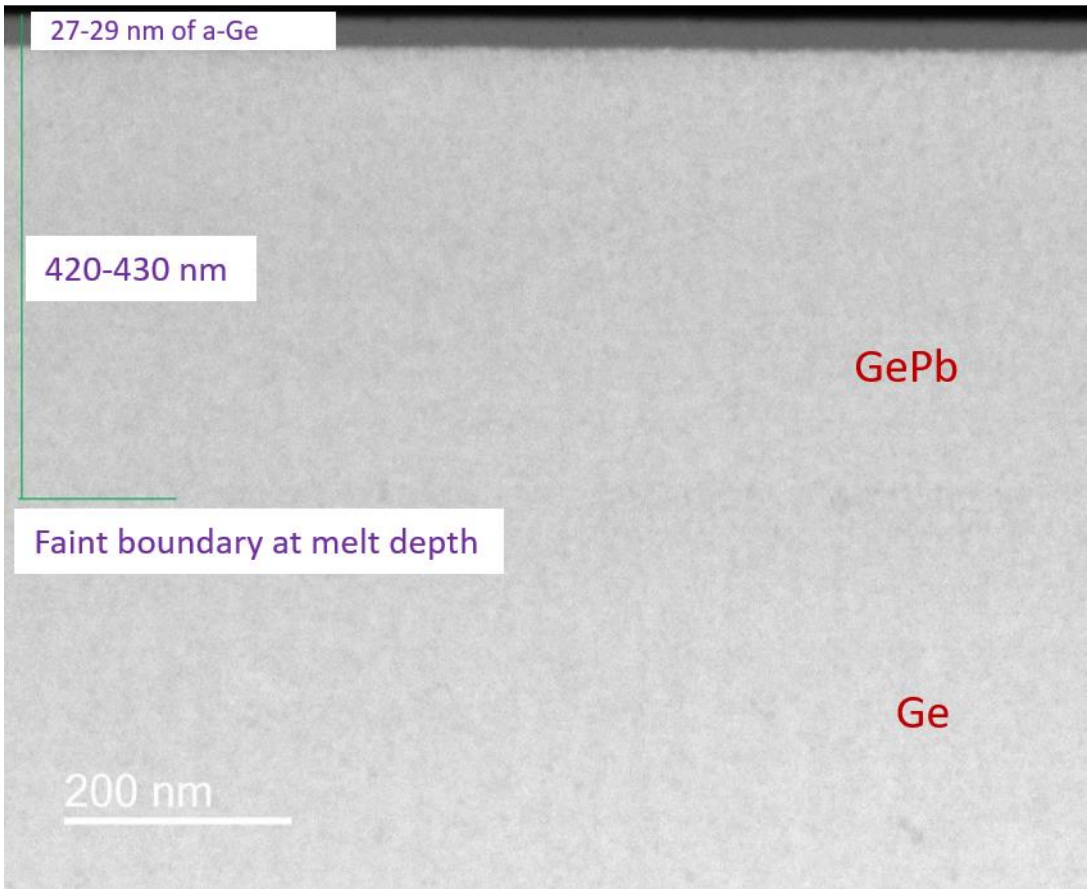

Fig. 10. *Cross-sectional bright field TEM micrograph of a 1x10^{15} cm^{-2} Pb implant into Ge at 800 keV after PLM.*

The highest Pb dose sample (5x10^{15} cm^{-2}) was also examined by both RSB/channelling and TEM to establish whether higher Pb content alloys could be produced. Fig. 13 shows RBS/channelling spectra for this sample after implantation and following PLM. The blue curve is a channelled spectrum after implantation showing an amorphous layer of around 440 nm, and the as-implanted Pb profile is shown in the magnified insert. After PLM, the channelled curve (pink) is significantly displaced from the Ge reference (red curve) and indicates that there is certainly a level of residual defects in this layer following PLM.

Comparing the Pb profiles from the insert figure, the channelled (pink) spectrum and the random (black) spectrum are almost identical, indicating little Pb substitutionality in this case. The Pb profile shape indicates that about ¼ of the Pb is segregated to the surface during PLM but the rest is trapped in the solid in (random) non-substitutional sites. This somewhat unusual behaviour can be understood by comparing with PLM studies of low solubility species in Si. For example, Au implanted Si behaves similarly during PLM [2], where higher Au doses cause breakdown of the liquid phase epitaxial growth following PLM, resulting in lateral segregation of Au into filaments that are rich in Au. We believe that this has occurred also for Pb in Ge during PLM, and, if so, it is a phenomenon that has never previously been observed. However, TEM is necessary to confirm such behaviour. Preliminary TEM has been undertaken but there appears to be a problem with sample preparation, and it has, thus far, not been possible to observe the residual defects in this sample after PLM.

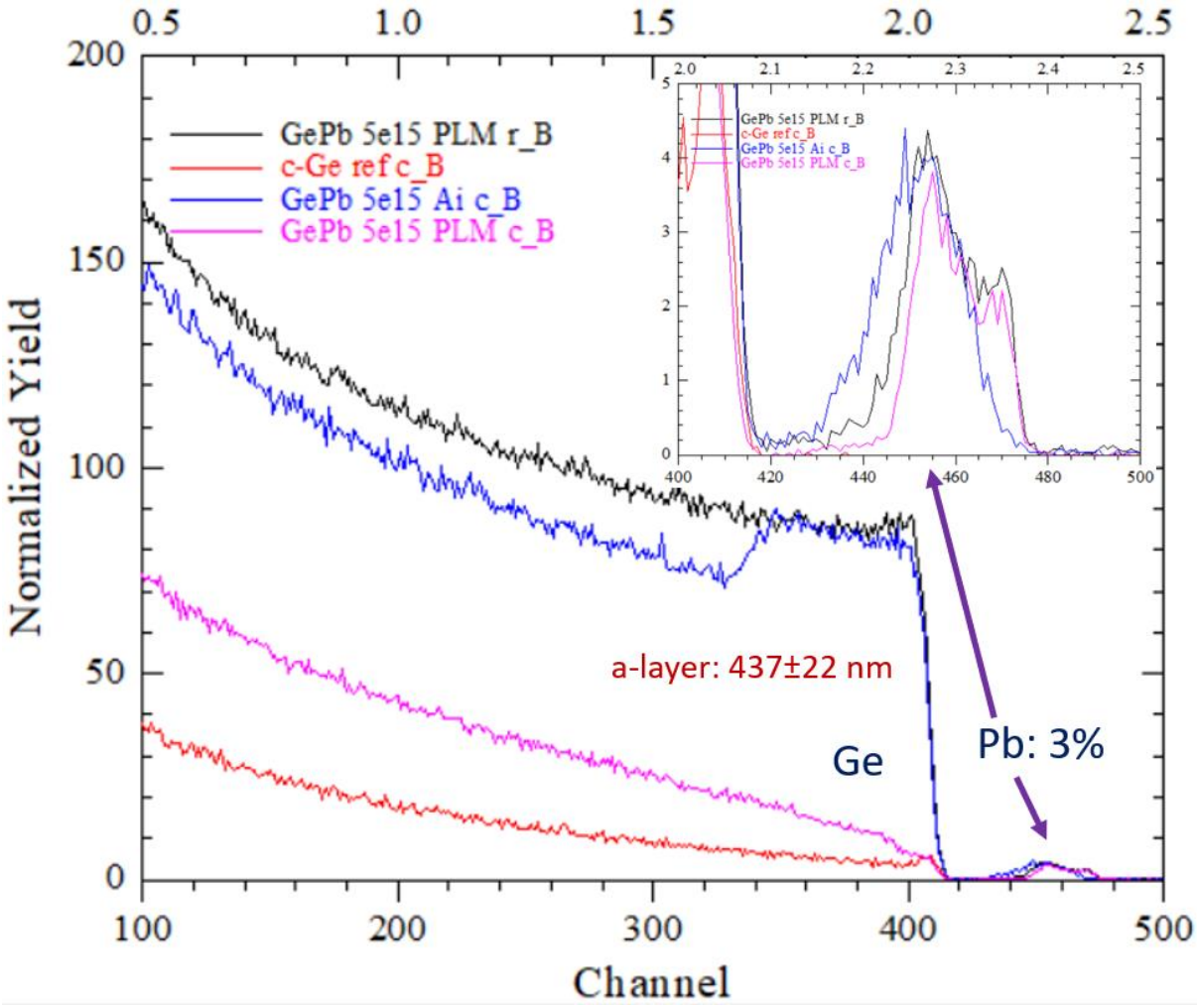

Fig. 11. *RBS random and channelled spectra for a 5x10^{15} cm^{-2} Pb implant into Ge at 800 keV before and after PLM, showing: a channelled spectrum for a Ge reference sample (red); a channelled spectrum after implantation (blue); a random spectrum after PLM (black); and a channelled spectrum after PLM (pink). The insert shows a magnified region of the Pb profiles for each spectrum.*

In summary, the GePb results obtained are extremely interesting and never before reported. When we are able to obtain TEM of the high dose Pb implant case, this work should be written up for publication.

3. Conclusion and Priorities for future work

Significant progress has been achieved on this project, despite issues with laboratory access due to 3 separate COVID lockdowns and down time of the PLM system at the US Army Benet Labs. The following achievements are noteworthy:

1. Characterisation of the CVD-grown samples on Si (and Ge) with several different analysis methods has proven to be very successful, with good agreement between the various techniques. A paper is currently in the final stages of preparation for publication on this work.
2. Preliminary work on the use of implantation to dope GeSn layers n-type has begun and the method of Sb implantation followed by PLM appears to be feasible, although the experimental design needs to be tweaked somewhat in a next iteration.
3. For the superlattice studies, RBS/channelling and TEM have been used to successfully characterise CVD-grown GeSn-Ge multilayers grown on both Ge and Si substrates. The TEM results, although extremely informative, are not quite up to publication quality and need to be repeated prior to expected publication of this work.
4. The efforts to reduce defect density and improve the quality of relaxed GeSn layers produced by both CVD and implant/PLM have not to date proven successful. However, the impediments to this approach have been identified, and a pathway for such experiments has been developed, particularly involving considerably thicker starting GeSn alloys.
5. The differences between the relaxation-induced defects in CVD-grown and implant/PLM Ge-Sn layers of similar composition have been identified, and, without much further TEM analysis, it will be possible to publish this work.
6. Initial studies to fabricate GePb alloys have provided much new data, including the first dilute GePb alloys ever produced. Following a repeat of some TEM data, an initial publication will be possible.

In terms of future work, that will extend beyond the end of the current project and is expected to be part of a new grant, the following will be the direction of study:

- Complete and submit a manuscript for publication on characterisation of various compositions of GeSn grown on Si by CVD.
- Further attempts will be made to successfully implement the PLM re-melting strategy on CVD-grown GeSn on Si in an attempt to reduce defect density. However, this will require thicker GeSn films, greater than about 800 nm, and some tweaking of the experimental approach.
- Assess the data to date on CVD-grown superlattices on both Ge and Si and undertake any further work that is required to publish it (including annealing to fully relax the films). Certainly, further TEM will be required to eliminate the FIB damage in existing TEM samples. Write up the data for publication.

- Undertake further fabrication of Sb implanted shallow n-type layers on CVD-grown GeSn and undertake PLM. Carry out electrical measurements to fully assess layers. Use this data to fabricate n-type layers and photodetector device structures.
- Based on the results to date, use Raman mapping to obtain a simple measure of the defect density from peak shifts, and undertake etching studies to correlate defect density with depth in CVD-grown GeSn films on Si, including the effect of graded buffer layers on defect reduction. TEM will be important to 'calibrate' the Raman defects levels.
- Based on the very successful preliminary studies of Pb implanted Ge and subsequent PLM, publish these initial results, following a little further TEM analysis. Further develop this technology for a range of implanted Pb doses (Pb concentrations) and PLM fluences. Fully assess the GePb films.
- Thermally anneal all GeSn and GePb alloy films to assess their thermal stability and degree of strain relaxation.

References:

1. T. T. Tran, Q. Hudspeth, Y. Liu, L. A. Smillie, B. Wang, R. A. Bruce, J. Mathews, J. M. Warrender, J.S. Williams, Mat. Sci. Eng. **B 262**, 114702 (2020).
2. W. Yang, A. J. Akey, L. A. Smillie, J. P. Mailoa, B. C. Johnson, J. C. McCallum, D. Macdonald, T. Buonassisi, M. J. Aziz, and J. S. Williams, Phys. Rev. Mat. **1**, 074602 (2017)